



Parameter optimization in the friction stir welding of polycarbonate using cylindrical and conical tool pins

Leonardo Viana Dias^{1,2} · Aderci de Freitas Filho² · Cláudio Turani Vaz²

Received: 7 December 2021 / Accepted: 6 June 2022 / Published online: 30 June 2022

© The Author(s), under exclusive licence to The Brazilian Society of Mechanical Sciences and Engineering 2022

Abstract

The increasing use of polymeric materials, especially in structural applications, has created a demand for larger and more complex parts that must fulfill several requirements. Although polymers have high processability, properties such as low melting temperature, thermal conductivity, diffusion capability, and wettability, together with a wide variety of grades and mixtures, render the production of adequate welds difficult. Among the many polymeric welding processes, one of the most recent ones is friction stir welding, which is based on the heating and mixing of materials resulting from the friction between a rotating non-consumable tool and base material. Therefore, in the present study, the integrity of friction-stir-welded polycarbonate plates was investigated, and the welding parameters, tool pin profile, and temperature were correlated with the mechanical behavior of the welded joint. Welding was successfully performed, and a maximum ultimate tensile strength of 34 MPa was achieved with the conical pin profile. Increased friction played an important role in the mixing and maintenance of the plate thickness at the welding section. By plotting the ultimate tensile strength relative to the ratio of the rotation and transverse speed, it was possible to determine the optimum polycarbonate FSW parameters for each tool.

Keywords Welding · Friction · Polymer · Polycarbonate

1 Introduction

Polymer processing by welding presents significant challenges. Properties such as low superficial energy and wettability are problematic when traditional welding techniques based on melting and material addition [1] are applied. Depending on the heat source characteristics, adequate fusion control is difficult because of low thermal conductivity, melting, and degradation temperatures, which can result in discontinuities, such as a lack of fusion at the interface [2]. Furthermore, the same polymeric grade can have different molecular weights, additives, and processing routes,

which may lead to differences in important properties such as the melt flow index of the material. These features complicate the production of large polymeric structures with high productivity. This can be overcome by developing new processes such as friction stir welding (FSW), which is based on the use of a rapidly rotating non-consumable tool that is inserted into a rigidly fixed plate. After insertion, this tool is moved along the plate to heat and mix the material, thereby promoting joining without melting. FSW generates a lower heat input, which promotes fewer distortions, and prevents discontinuities such as solid inclusions. The lower energy consumption and higher productivity owing to the easy automation also render it an economically competitive process [3].

According to Pires et al. [4] and Commin et al. [5], although FSW was developed for the welding of low-density metals, such as aluminum and magnesium, its use has been expanded to other materials, such as carbon steel [6], high carbon steel [7], and stainless steel [8], with satisfactory results. Additionally, FSW has been successfully used as a processing tool, known as friction stir processing, to improve material properties by microstructural modification, alloy addition, and composite production

Technical Editor: Izabel Fernanda Machado.

✉ Cláudio Turani Vaz
claudioturani@gmail.com

¹ Instituto Federal de Educação Ciência e Tecnologia de Minas Gerais, Campus Ouro Branco, Ouro Branco, Minas Gerais, Brasil

² Centro Federal de Educação Tecnológica de Minas Gerais, Programa de Pós-Graduação em Engenharia de Materiais, Belo Horizonte, Minas Gerais, Brasil

[9]. Mirjavadi et al. [10] evaluated the performance of composites produced by TiO_2 nanoparticle addition in a metallic substrate (AA5083). Qiao et al. [11] investigated the mechanical behavior of composites produced by ZrO_2 addition in a magnesium matrix. In addition, Doniavi et al. [12] evaluated the mechanical properties of polycarbonate matrix composites with aluminum oxide nanoparticles.

In the field of polymeric materials, several efforts have been made by researchers to understand and overcome the challenges associated with the FSW of polymers. Similar to solid-state welding, the most important phenomenon is diffusion, which is complicated by the macromolecular nature of polymers [13] [14]. The entangled macromolecular structure of the polymers has a diffusion coefficient magnitude of approximately $10^{-16} \text{ m}^2/\text{s}$, different from that of metallic alloys, which have a diffusion coefficient of approximately $10^{-5} \text{ m}^2/\text{s}$ [15]. Nevertheless, promising results have already been obtained in the FSW of polymeric materials. For example, Panneerselvam and Lenin [16] obtained adequate mechanical properties by joining nylon 6 using FSW with a tool equipped with a threaded pin. Hoseinlghab et al. [17] also achieved satisfactory results by obtaining properties similar to those of the base material used for welding high-density polyethylene. These results have prompted research studies on the relationship between the mechanical behavior and process parameters (transverse and rotation speeds and tool pin geometry) of the weld, which have not yet been completely explained.

The present study aimed to investigate the application of FSW to polycarbonate sheets. The effects of tool rotation and transverse speed during on-plate welding were investigated using cylindrical and conical tool pin profiles. Temperature data were obtained, and morphological analyses and tensile

tests were performed to obtain the optimum parameters for material welding.

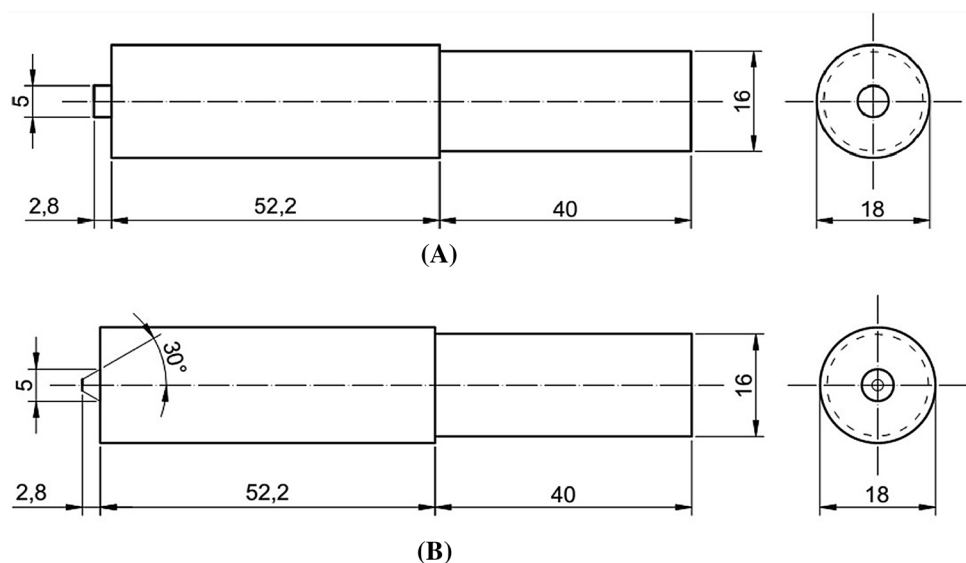
2 Materials and methods

Commercial polycarbonate sheets, namely LEXAN THERMOCLEAR from SABIC Innovative Plastics, were used in this study. This polymer is widely used in the civil industry, and its application in other industries, such as the automotive and aerospace industries, is increasing owing to its tenacity, transparency, and adequate heat resistance [18]. The sheets had a thickness of 3 mm and were cut into dimensions of $178 \times 120 \text{ mm}$. Before welding, the polymer was subjected to tensile testing and differential scanning calorimetry (DSC). The ultimate tensile strength (UTS) was 62 MPa, and the glass transition temperature (T_g) according to the DSC results was $150 \text{ }^\circ\text{C}$.

The welding tool was made of AISI H13 steel, which has been successfully used by Sahu et al. [19] and Zafar et al. [20] previously. This steel grade possesses wear resistance and adequate machinability and is also used in hot work applications. A design of the tool is illustrated in Fig. 1. Cylindrical tools were used by Arici and Selale [21] with moderate success during the FSW of polyethylene, whereas a conical tool pin was successfully used by Derazkola et al. [22] during polycarbonate welding. Sadeghian and Givi [23] compared both tool pin profiles for acrylonitrile–butadiene–styrene and found the relative strength for each tool profile to be approximately 99.1% and 100.4%, respectively.

Welding was performed in a CLEVER FH-4 milling machine using a fixture apparatus with six clamps (Fig. 2) assembled on the milling trail to rigidly position the polycarbonate sheets.

Fig. 1 Friction stir welding tool project with a cylindrical and b conical pins



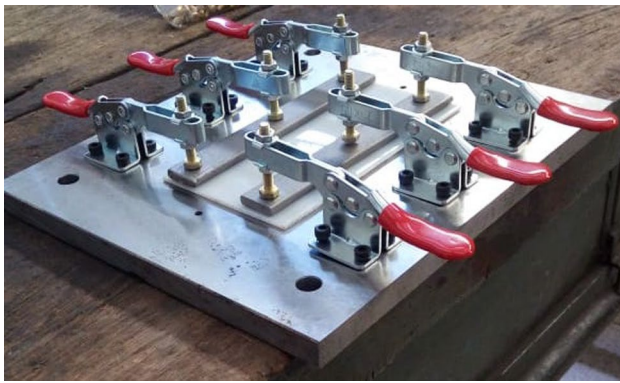


Fig. 2 Fixture apparatus used in this study

Table 1 Experimental parameters for the FSW tests

Tool Pin	Transverse speed (mm/min)	Rotation speed (RPM)
Cylindrical	25	466
		1176
		2160
	40	466
		1176
		2160
Conical	25	466
		1176
		2160
	40	466
		1176
		2160

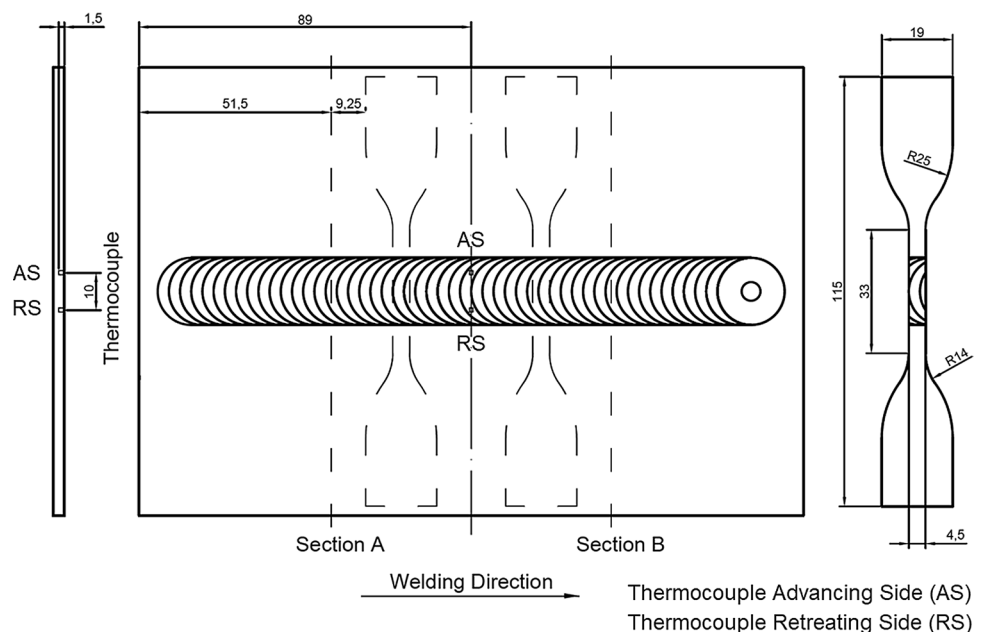
The welds were made using 3° tilt angles in the welding direction to avoid material pool-out during welding and increase the axial force. A tool penetration of 2.8 mm was achieved for adequate surface contact between the tool shoulder and material. Table 1 lists the welding and rotation speeds that were previously validated by preliminary welding tests. Parameter selection was based on the results of previously published work [24] in which the process parameters (transverse and rotation speed) were compared to the weld mechanical performance.

During welding, the temperature data were obtained using type K thermocouples. The thermocouples were positioned 1.5 mm from the bottom of the sheets to avoid interference with the mixing material on both sides (advancing and retreating) of the welding bead, as indicated in Fig. 3.

The presence of superficial defects was verified by visual evaluation. Due to the material transparency, a dark background was used to improve contrast. The images were capturing using a Cannon EOS Rebel T100 camera with an 18–55-mm lens. To evaluate the welding morphology, two cuts were made in the transverse direction of the plate. The samples were sanded with 120 to #3000 sandpapers and polished with suspended alumina as an abrasive. The images were captured using a Canon EOS Rebel T100 camera with a Tokina 100 mm F/2.8 macro lens.

The tensile strength samples were cut according to ASTM D-638. Two samples were obtained from each plate (a total of six specimens for each condition), avoiding the start and end of the weld bead. All cuts were made using water to avoid heating, which can affect the morphology and properties of the base material and weld. The tensile tests were performed using an EMIC DL30000N machine with a Trd

Fig. 3 Thermocouple position, cutting section of the plate, and tensile sample dimensions



29 load cell and a test velocity of 1 mm/min. The fracture position and characteristics were visually examined using a negatoscope. The position of the tensile test specimen is also demonstrated in Fig. 3.

To analyze the influence of each parameter on the UTS results, analysis of variance (ANOVA) was performed using MINITAB software.

3 Results and discussion

All samples were successfully processed by FSW. However, significant differences in the mixing quality and final properties of the polycarbonate sheets were observed. Figure 4 shows the top and bottom weld bead views produced with a transverse speed of 25 mm/min and rotation speeds of 466 and 2160 RPM using the cylindrical and conical toll pins. The top surface, at higher rotation speeds, became opaque and also presented a less brittle flash for both tools. Owing to the polycarbonate transparency, it was possible to observe the root quality at the back surface. In addition to the difference in the area mixed by the pin, the welding bead prepared with the conical pin profile appears to be more homogeneous than that prepared with the cylindrical pin profile. For the different parameters, the change in transverse speed did not result in significant, visually apparent modifications.

The cross-sectional images (Fig. 5) show a visible reduction in the plate thickness, especially when the welding was performed at the lowest rotation speed of 466 RPM. Few root defects are mainly observed at the interface between

the welding nugget and plate at the advancing side. For both tools, increasing the rotation speed resulted in a larger mixing area and more symmetrical cross section. In addition, the conical pin profile promotes a narrow root.

The variations mentioned above were confirmed using the graphs shown in Fig. 6, which presents the mixing and missing material areas measured from the cross-sectional images as functions of the rotation and transverse speeds for different tool geometries.

Using the thermocouple data collected, a graph was constructed by plotting the average temperature obtained for each parameter as a function of time (Fig. 7). As the thermocouple position was the same for every sample, the transverse speed increase resulted in a faster approach of the welding tool to the thermocouple, starting the area heating earlier. In addition, the cooling rate was not significantly affected.

Figure 8 shows the average peak temperature as a function of the rotation and transverse speeds for the cylindrical and conical pin profiles. An increase in the rotation speed resulted in an increase in the peak temperature, whereas an increase in the transverse speed resulted in temperature reduction. Notably, the average peak temperature with the conical tool pin was lower than that with the cylindrical tool pin.

The tensile test results allowed for a comparison of the mechanical properties of the polycarbonate welds prepared with the FSW process employing different parameters. Using a cylindrical tool, an increase in the rotation speed directly improved the UTS; however, when using the conical tool,

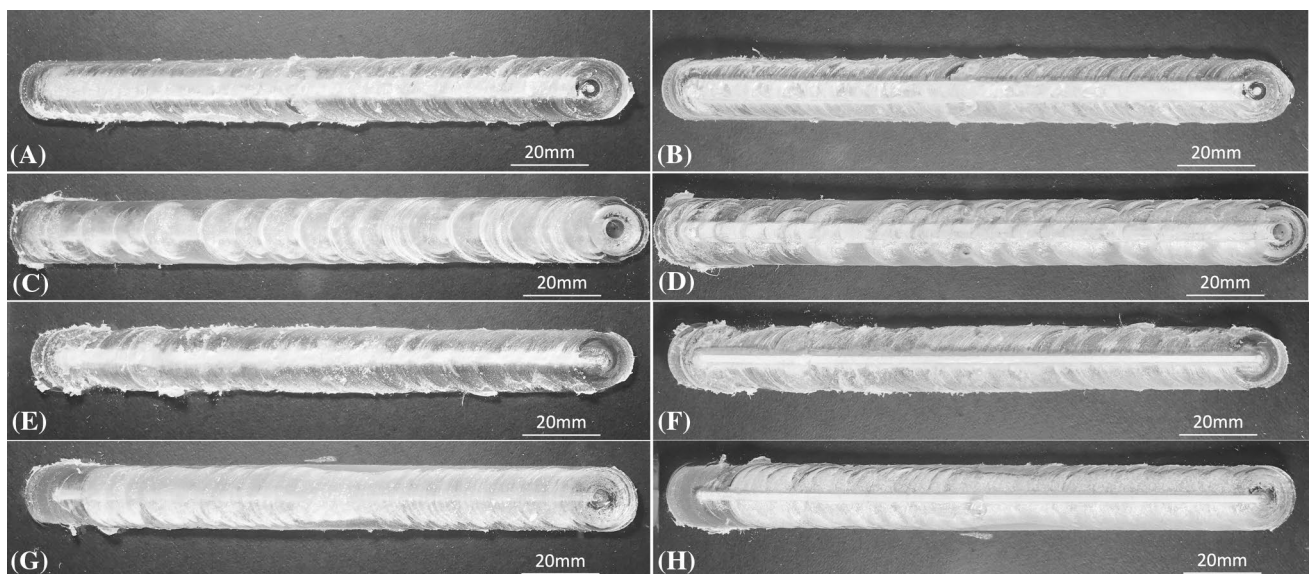


Fig. 4 Weld bead of polycarbonate sheets welded using **a** 466 RPM with a cylindrical tool pin, **b** 466 RPM with a cylindrical tool pin, **c** 2160 RPM with a cylindrical tool pin, **d** 2160 RPM with a cylindrical

tool pin, **e** 466 RPM with a conical tool pin, **f** 466 RPM with a conical tool pin, **g** 2160 RPM with a conical tool pin, and **h** 2160 RPM with a conical tool pin

Fig. 5 Cross section of the friction-stir-welded plates using **a** 466 RPM 40 mm/min cylindrical pin, **b** 466 RPM 40 mm/min conical pin, **c** 2160 RPM 40 mm/min cylindrical pin, and **d** 2160 RPM 40 mm/min conical tool pin profiles

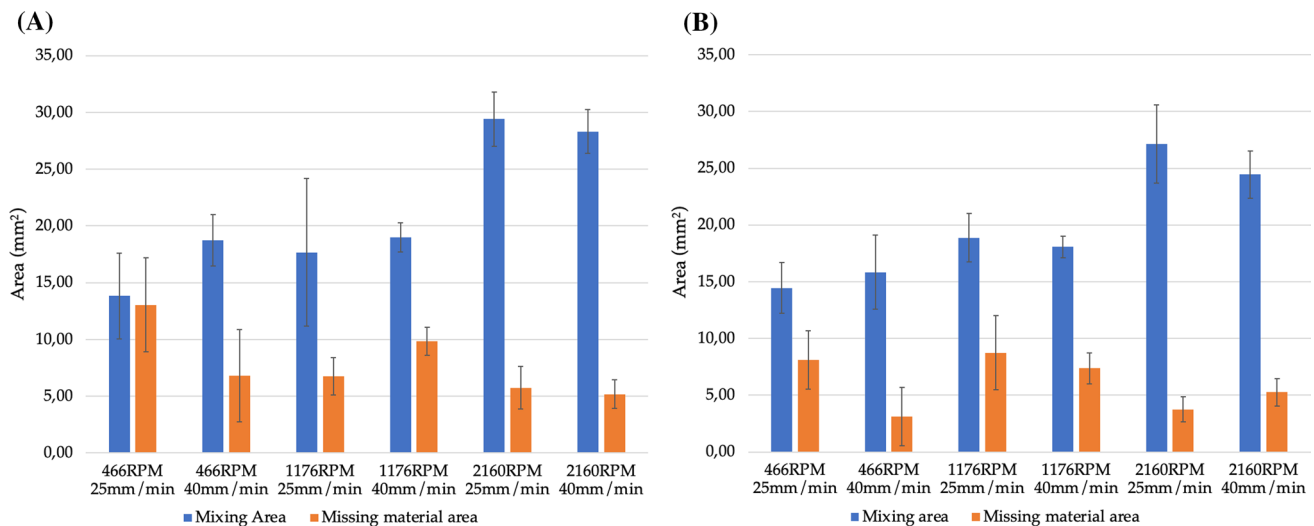
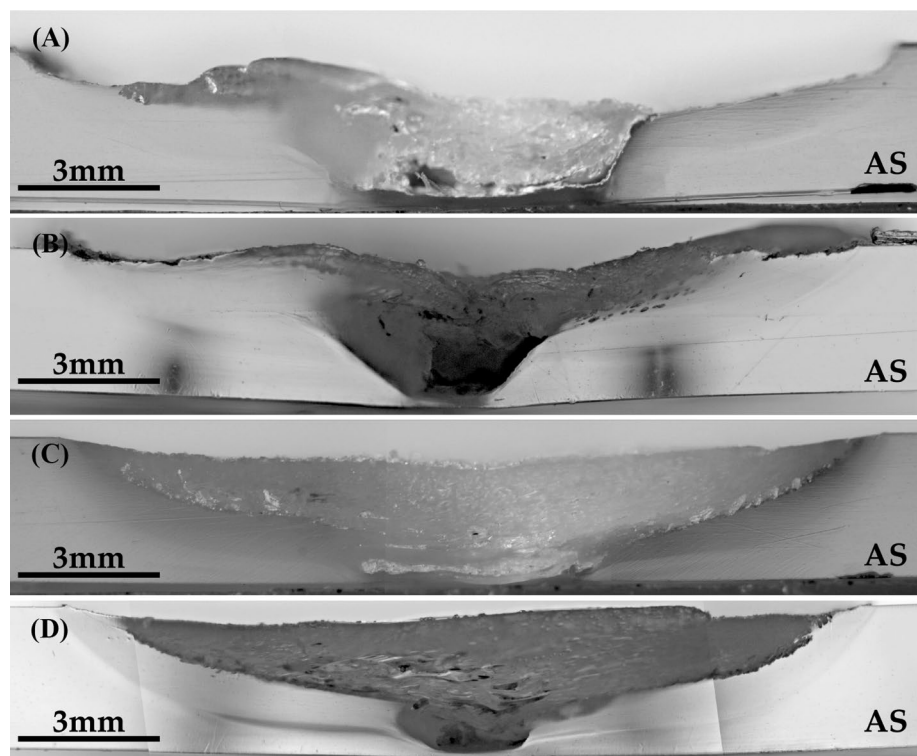


Fig. 6 Morphology data of the cross section of the welded polycarbonate sheets using **a** cylindrical and **b** conical tool pin profiles

intermediate (1176 RPM) and maximum rotation speeds (2160 RPM) resulted in a higher UTS, as shown in Table 2.

Another important piece of information obtained from the tensile test is the fracture location. For rotation speeds of 466 RPM and 1176 RPM, the fracture was located at the intersection of the weld nugget and thermomechanically affected zone at the advancing side, as shown in Fig. 9. At the maximum rotation speed (2160 RPM), some ruptures remained at this interface, which were mainly

observed across the thermomechanically affected zone and at the interface between it and the base material. The same behavior was observed [13, 20] when welding nylon 6 and poly(methyl methacrylate).

The highest UTS obtained was 34 MPa when welding using a conical tool pin with a rotation speed of 2160 RPM and transverse speed of 40 mm/min, corresponding to 55% of the UTS of polycarbonate. Shazly et al. [13] and Derazkola et al. [22] reported values of 30.78% and 82%, respectively,

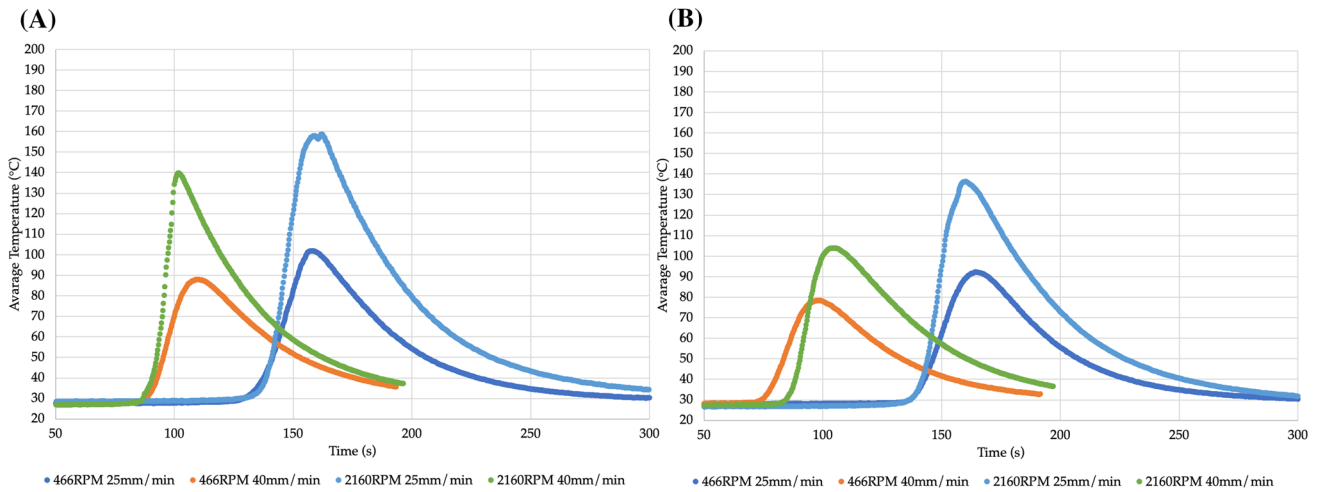


Fig. 7 Graphical representation of the average heating temperature per welding time using a cylindrical and b conical tool pin profiles

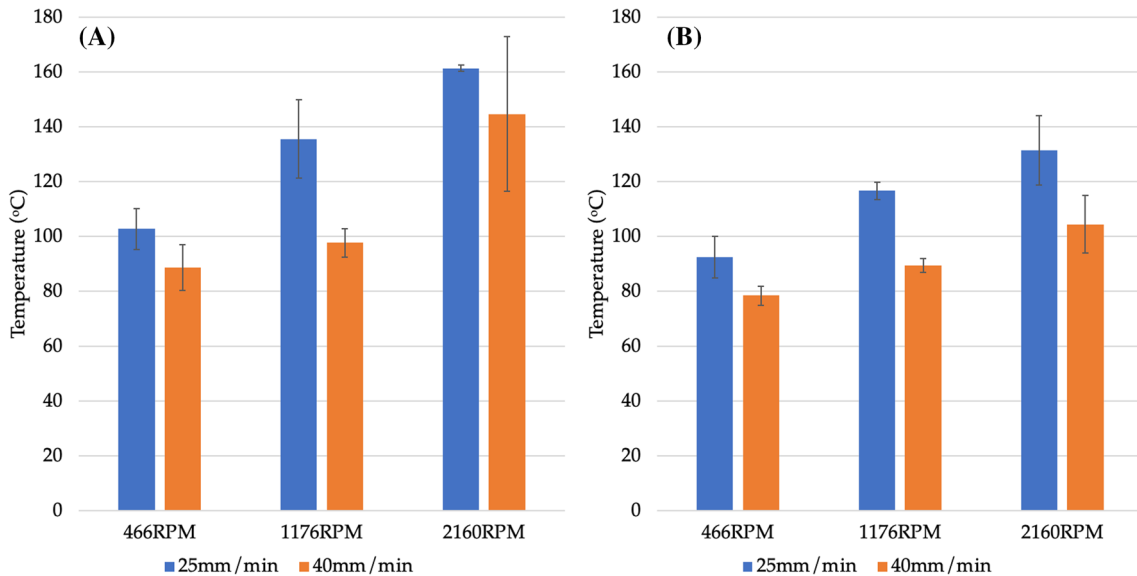


Fig. 8 Graphical representation of the average peak temperature for each parameter using a cylindrical and b conical tool pin profiles

compared with the base polymer. A strength decrease, especially for an on-plate friction stir weld, is expected even with optimum parameters due to, for example, the addition of materials to change the base material properties, thickness reduction, and mass loss resulting from flash defects and polymeric degradation [20]. Another important reason for a reduction in UTS compared with the base material is the tunnel defects visible in almost all cross sections, especially for the conical pin profile, resulting in a lack of material at the root interface. However, the average UTS results were higher for the conical tool pin profile compared with that of the cylindrical tool pin profile at the same parameters, which can be attributed to the smaller volume of mixed material in the weld preserving the original plate and its properties.

Only the cylindrical pin profile at 2160 RPM and 25 mm/min raised the plate temperature above the T_g at the thermocouple position (2.5 mm away from the tool pin). Reaching T_g at the mixing zone is fundamental to creating a wider segmental movement, allowing the material to flow and mix properly, thereby leading to a transition from a “solid-state” to a “rubbery state” welding, as suggested by Dias and Vaz [24]. When increasing the rotation speed, and consequently the temperature, the average pullout material also reduced, thereby maintaining the plate thickness at the welding section. However, it is important to note that peak friction can be achieved before significant material degradation.

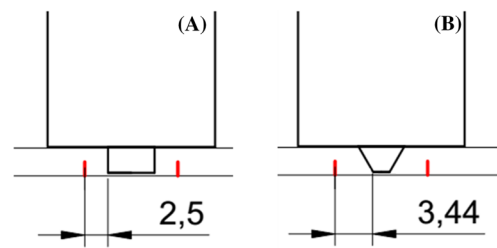
The conical pin profile also decreased the measured temperature; however, this was because of the distance between

Table 2 Average ultimate tensile strength obtained using different FSW parameters

	Cylindrical tool pin profile		Conical tool pin profile	
	UTS (MPa)	Std Dev	UTS (MPa)	Std Dev
466 RPM 25 mm/min	12.1	3.0	19.3	2.8
466 RPM 40 mm/min	10.9	3.5	18.3	1.6
1176 RPM 25 mm/min	24.6	4.9	30.7	1.1
1176 RPM 40 mm/min	19.3	1.7	20.8	2.6
2160 RPM 25 mm/min	30.2	2.2	29.0	2.0
2160 RPM 40 mm/min	30.6	4.0	34.0	3.1

the thermocouple position and the pin as a result of its profile (Fig. 10). Therefore, although the shoulder contributed significantly to heating [25] [26], the pin also plays an important role in heating, especially for polymers with low conductivity.

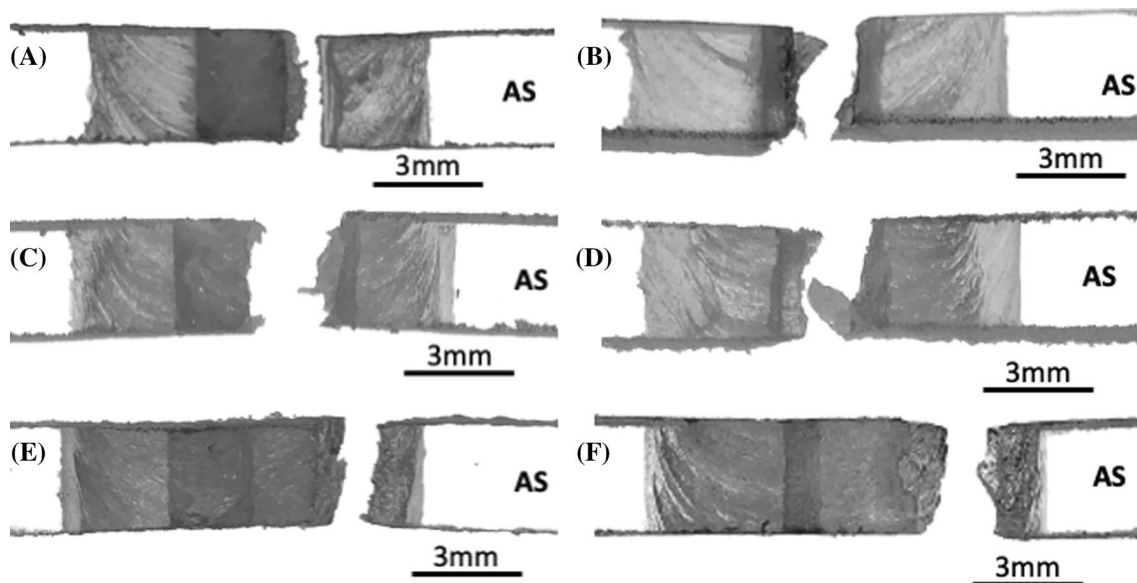
Interaction plots (Fig. 11) indicate that the welds produced with a conical pin exhibit a higher UTS than those produced with a cylindrical pin. Increasing the rotation speed also resulted in an increase in the average UTS for both tools, whereas an increase in the transverse speed at low rotation speeds resulted in lower UTS values. However, at 2160 RPM, the graphs indicate that the optimal transverse

**Fig. 10** Schematics of the distance between the thermocouple position and tool pin surface for **a** cylindrical and **b** conical pin profiles

speed is 40 mm/min. This is because of high rotation speeds leading to overheating and material degradation, which is generally compensated for by the transverse speed.

To understand the combined influence of rotation (R) and welding or transverse (T) speed on the weld UTS, a graph was constructed plotting UTS as a function of the R/T ratio (Fig. 12). For both tools, the graphs approach a second-degree polynomial equation, where the maximum UTS values represent the optimum parameter (rotation and transverse speed) combination.

By calculating the equation derivative, it is possible to determine the optimal R/T ratio to produce the optimum weld using a specific material and tool. Consequently, maximum productivity can be achieved by combining the transverse with the rotation speed so that the optimum R/T ratio, as calculated from the graph, is maintained. For the cylindrical and conical tool, the optimum R/T ratio obtained in this study was 78.2 and 65.5, respectively,

**Fig. 9** Fractured tensile samples using **a** 466 RPM and 25 mm/min cylindrical, **b** 466 RPM and 25 mm/min conical, **c** 1176 RPM and 25 mm/min cylindrical, **d** 1176 RPM and 25 mm/min conical, **e** 2160 RPM and 25 mm/min cylindrical, and **f** 2160 RPM and 25 mm/min conical tools

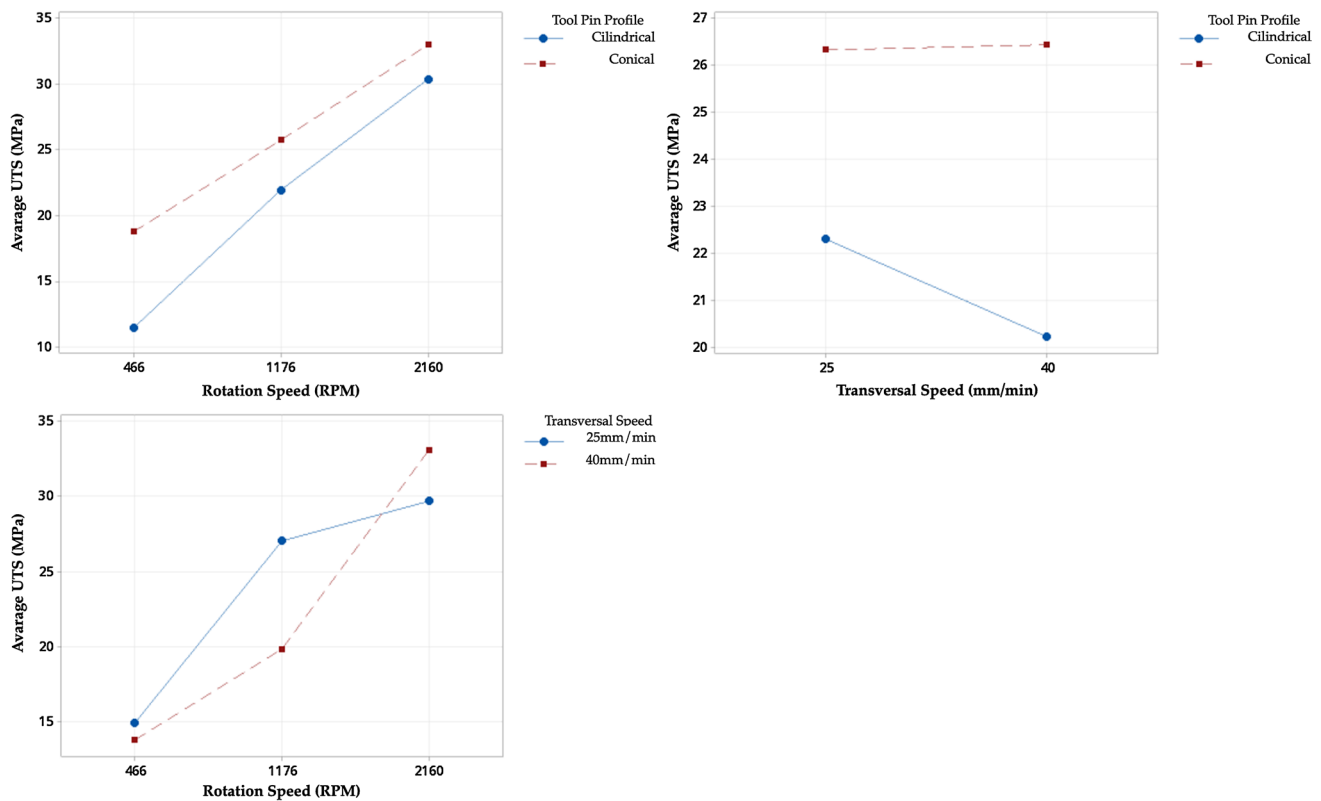


Fig. 11 ANOVA

indicating that the latter required less friction than the former.

Tool profile changes require specific parameters for different materials. Plate thickness, material properties, and tool surface contact are some of the variables that must be considered before choosing a tool. Hajideh et al. [27] indicated that the tool geometry has a greater effect on the mechanical properties of the friction-stir-welded joint than other parameters. Hoseinlghab et al. [17] concluded that the effects of the pin geometry on the weld are independent of those of the parameters. Therefore, the UTS as a function of the R/T ratio graph is an important tool when choosing the optimal parameters for a material with the same tool-shoulder dimensions and proportional pin length.

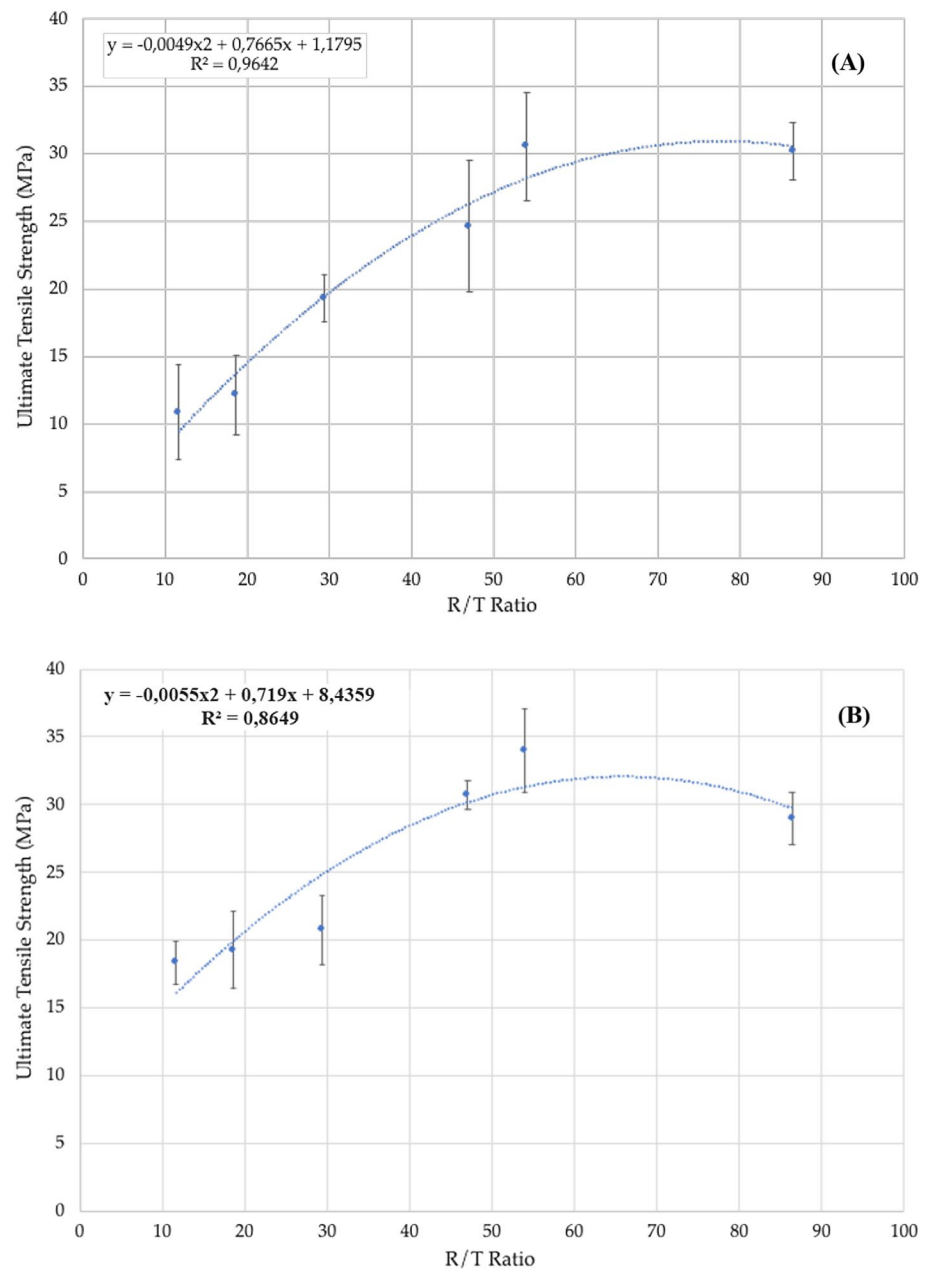
4 Conclusions

This study aimed to investigate the influence of FSW parameter optimization on the visual aspects and mechanical properties of polycarbonate and evaluate the temperatures that can be reached using the optimal combinations. The

following conclusions were drawn from the experimental results.

- The highest UTS obtained for on-plate welding was 61% of the polycarbonate when using a conical tool pin profile.
- Although the conical pin profile produces more tunnel defects, it still results in a better average UTS.
- The pin profile plays an important role in plate heating.
- The rotation tool acts as a pulling material due to inadequate heat generation; therefore, reaching the glass transition temperature is important for adequate mixing and the preservation of the welding section thickness.
- The benefits of friction and temperature increases reach a maximum, after which the average UTS tends to decrease because of polymer degradation.
- The graph of UTS as a function of the R/T ratio indicates the optimal parameters that maximize productivity with a higher transverse speed. For the cylindrical and conical tools, the optimum R/T ratios obtained in this study were 78.2 and 65.5, respectively, indicating that the latter requires less friction than the former.

Fig. 12 Average UTS as a function of the R/T ratio for **a** cylindrical and **b** conical tool pin profiles



Funding information Coordenação de Aperfeiçoamento de Pessoal de Nível Superior

References

- Strand SR (2004) Effects of Friction Stir Welding on Polymer Microstructure. Brigham Young University, Provo
- Dashatan SH, Azdast T, Ahmadi SR, Bagheri A (2013) Friction stir spot welding of dissimilar polymethyl methacrylate and acrylonitrile butadiene styrene sheets. *Mater Des* 45:135–141. <https://doi.org/10.1016/j.matdes.2012.08.071>
- Majeed T, Wahid MA, Alam MN, Mehta Y, Siddiquee AN (2021) Friction stir welding: a sustainable manufacturing process. *Mater Today Proc* 46(15):6558–6563. <https://doi.org/10.1016/j.matpr.2021.04.025>
- Pires JP, Cota BS, Bracarense AQ, Campolina BA (2018) Temperature distribution prediction in 5052 H34 aluminum alloy joints welded by friction stir welding process. *Soldag E Insp* 23(2):247–263. <https://doi.org/10.1590/0104-9224/S12302.11>
- Commin L, Dumont M, Masse JE, Barrallier L (2009) Friction stir welding of AZ31 magnesium alloy rolled sheets: influence of processing parameters. *Acta Mater* 57(2):326–334. <https://doi.org/10.1016/j.actamat.2008.09.011>

6. Fujii H, Cui L, Tsuji N, Maeda M, Nakata K, Nogi K (2006) Friction stir welding of carbon steels. *Mater Sci Eng A* 429(1–2):50–57. <https://doi.org/10.1016/j.msea.2006.04.118>
7. Cui L, Fujii H, Tsuji N, Nogi K (2007) Friction stir welding of a high carbon steel. *Scripta Mater* 56(7):637–640. <https://doi.org/10.1016/j.scriptamat.2006.12.004>
8. Andrade TC et al (2015) Microestrutura de uma solda dissimilar entre o aço inoxidável ferrítico AISI 410S e o aço inoxidável austenítico AISI 304L soldado pelo processo FSW. *Soldag E Insp* 20(4):467–478. <https://doi.org/10.1590/0104-9224/SI2004.13>
9. Weglowski MS (2018) Friction stir processing – State of the art. *Arch Civil Mech Eng* 18:114–129. <https://doi.org/10.1016/j.acme.2017.06.002>
10. Mirjavadi SS, Alipour M, Emamian S, Kord S, Hamouda AMS, Koppad PG, Keshavamurthy R (2017) Influence of TiO₂ nanoparticles incorporation to friction stir welded 5083 aluminum alloy on the microstructure, mechanical properties and wear resistance. *J Alloy Compd* 712:795–803. <https://doi.org/10.1016/j.jallcom.2017.04.114>
11. Qiao K, Zhang T, Wang K, Yuan S, Wang L, Chen S, Wang Y, Xue K, Wang W (2022) Effect of multi-pass friction stir processing on the microstructure evolution and corrosion behavior of ZrO₂/AZ31 magnesium matrix composite. *J Market Res* 18:1166–1179. <https://doi.org/10.1016/j.jmrt.2022.02.127>
12. Doniavi A, Babazadeh S, Azdast T, Hasanzadeh R (2017) An investigation on the mechanical properties of friction stir welded polycarbonate/aluminium oxide nanocomposite sheets. *J Elastom Plast* 49(6):498–512. <https://doi.org/10.1177/0095244316674352>
13. Shazly M, Ahmed MMZ, El-Raey M (2014) Friction stir welding of polycarbonate sheets. *TMS Annu Meet*. <https://doi.org/10.1002/9781118888056.ch65>
14. Gao J, Li C, Shilpakar U, Shen Y (2015) Improvements of mechanical properties in dissimilar joints of HDPE and ABS via carbon nanotubes during friction stir welding process. *Mater Des* 86:289–296. <https://doi.org/10.1016/j.matdes.2015.07.095>
15. Kausch HH, Tirrell M (1989) Polymer interdiffusion. *Annu Rev Mater Sci* 19:341–377. <https://doi.org/10.1146/annurev.ms.19.080189.002013>
16. Panneerselvam K, Lenin K (2014) Joining of nylon 6 plate by friction stir welding process using threaded pin profile. *Mater Des* 53:302–307. <https://doi.org/10.1016/j.matdes.2013.07.017>
17. Hoseinlghab S, Mirjavadi SS, Sadeghian N, Jalili I, Azarbarmas M, Besharati Givi MK (2015) Influences of welding parameters on the quality and creep properties of friction stir welded polyethylene plates. *Mater Des* 67:369–378. <https://doi.org/10.1016/j.matdes.2014.11.039>
18. Wiebeck HJ, Harada J (2005) Plásticos de engenharia: tecnologia e Aplicações. Artliber Ltda, São Paulo
19. Sahu SK et al (2018) Friction stir welding of polypropylene sheet. *Eng Sci Technol Int J* 21(2):245–254. <https://doi.org/10.1016/j.jestch.2018.03.002>
20. Zafar A, Awang M, Khan SR, Emamian S (2016) Investigating friction stir welding on thick nylon 6 plates. *Weld J* 95:210–218
21. Arici A, Selale S (2007) Effects of tool tilt angle on tensile strength and fracture locations of friction stir welding of polyethylene. *Sci Technol Weld Join* 12(6):536–539. <https://doi.org/10.1179/174329307X173706>
22. Derazkola HA, Simchi A, Lambiase F (2019) Friction stir welding of polycarbonate lap joints: relationship between processing parameters and mechanical properties. *Polym Test*. <https://doi.org/10.1016/j.polymertesting.2019.105999>
23. Sadeghian N, Givi MKB (2015) Experimental optimization of the mechanical properties of friction stir welded acrylonitrile butadiene styrene sheets. *Mater Des* 67:145–153. <https://doi.org/10.1016/j.matdes.2014.11.032>
24. Dias LV, Vaz CT (2021) União de termoplásticos pelo processo friction stir welding: influência da ferramenta e parâmetros do processo. *Soldag Insp*. <https://doi.org/10.1590/0104-9224/si25.41>
25. Nandan R, DebRoy T, Bhadeshia HKDH (2008) Recent advances in friction-stir welding - Process, weldment structure and properties. *Prog Mater Sci* 53(6):980–1023. <https://doi.org/10.1016/j.pmatsci.2008.05.001>
26. Zhang YN, Cao X, Larose S, Wanjara P (2012) Review of tools for friction stir welding and processing. *Can Metall Q* 51(3):250–261. <https://doi.org/10.1179/1879139512Y.0000000015>
27. Hajideh MR, Farahani M, Alavi SAD, Ramezani NM (2017) Investigation on the effects of tool geometry on the microstructure and the mechanical properties of dissimilar friction stir welded polyethylene and polypropylene sheets. *J Manuf Process* 26:269–279. <https://doi.org/10.1016/j.jmapro.2017.02.018>

Publisher's Note Springer Nature remains neutral with regard to jurisdictional claims in published maps and institutional affiliations.